ARTICLES
https://doi.org/10.1038/s41561-019-0372-0
nature geoscience

Hydrogeological constraints on the formation of Palaeoproterozoic banded iron formations

Leslie J. Robbins[1,8*], Sean P. Funk[1], Shannon L. Flynn[2], Tyler J. Warchola[1], Zhiquan Li[1,3,4], Stefan V. Lalonde[5], Benjamin J. Rostron[1], Albertus J. B. Smith[6,7], Nicolas J. Beukes[6,7], Michiel O. de Kock[6,7], Larry M. Heaman[1], Daniel S. Alessi[1] and Kurt O. Konhauser[1]

Banded iron formations are critical to track changes in Archaean to Palaeoproterozoic ocean chemistry, with deposition triggered by water column iron oxidation. Recently, however, it was suggested that reduced iron minerals were the primary precipitates, and these were subsequently oxidized by oxygen-bearing groundwater. If true, this would cast doubt on our understanding of how banded iron formations were deposited and their ability to record early ocean chemistry. Here we present a hydrogeological box model, based on the approximately 2.5 billion year old Hamersley Basin of Western Australia, developed to evaluate the plausibility of secondary iron oxidation. The box model calculates the time required for groundwater to flux enough oxygen through the basin to oxidize a given amount of ferrous iron. Less than 9% of nearly four million model iterations returned oxidation times less than the age of the basin. Successful simulations required simultaneously steep hydraulic gradients, high permeability and elevated oxygen concentrations. Our simulations show that the postdepositional oxidation of large banded iron formations is unlikely, except on a limited scale (that is, during secondary ore formation), and that oxidized iron phases were probably the precursor to large Palaeoproterozoic banded iron formations.

Among the largest banded iron formations (BIFs) are those of the Transvaal Supergroup in South Africa[1,2] and the Hamersley Basin in Western Australia[2,3]. The Transvaal Supergroup contains the ~2.52 to 2.43 billion years ago (Ga) Kuruman and Griquatown iron formations, as well as the correlative Penge Iron Formation, and has an aerial extent of ~110,000 km^2 and a maximum thickness of 950 m (refs. [1,2]). The Transvaal Supergroup can be correlated with the Hamersley Group in Western Australia[1] (Supplementary Fig. 1), which has an aerial extent of over 100,000 km^2, a thickness of ~2.5 km (for example, Morris[4]) and includes the Marra Mamba, Brockman, Weeli Wolli and Boolgeeda iron formations that were deposited between ~2.6 and 2.45 Ga. The peak deposition for both the South African and Australian BIFs[2] coincides with the onset of the Great Oxidation Event (GOE) at ~2.45 Ga (refs. [5,6]), when oxygen first accumulated in the atmosphere (reviewed in Farquhar et al.[7]).

Iron oxidation and BIF deposition

The ferric iron in BIFs is generally considered to have formed by the oxidation of dissolved ferrous iron, Fe(II), in seawater by either oxygen produced by cyanobacteria[8] or via anoxygenic photoferrotrophy[9]. In either case, the primary minerals deposited would be hydrous ferric oxyhydroxides (HFOs)[10]. The deposition of HFOs and the subsequent dehydration to haematite (Fe_2O_3) or reduction to magnetite (Fe_3O_4) and siderite ($FeCO_3$) is supported by mineral textures and petrographic relationships, stable isotopes and rare earth element patterns (reviewed in Konhauser et al.[11]).

Recently, greenalite ($Fe_3Si_2O_5(OH)_4$), an Fe(II) silicate mineral, was interpreted in some Transvaal Supergroup and Hamersley Group BIF as a water column precipitate that constituted the precursor to BIFs[12–15] (Fig. 1). If true, this would have significant implications for Archaean and Palaeoproterozoic seawater chemistry, as the interpretation of the BIF trace element archive is based on the predictable nature of the adsorption to HFOs that would have precipitated from, and equilibrated with, contemporaneous seawater[16,17]. Crucially, it implies the lack of an Fe(II) oxidant and a marine photic zone biosphere at that time. This is clearly at odds with the widely accepted view that the Neoarchaean oceans were already oxygenated and a diverse marine biota that consisted of cyanobacteria and anoxygenic phototrophs was already in existence[18].

Nonetheless, intrigued by the possibility of a greenalite precursor (Fig. 1) and that a significant departure in our understanding of Archaean–Palaeoproterozoic ocean chemistry and the biosphere would be required, we modelled the feasibility of having secondary fluids oxidize an Fe(II) precursor at a basin scale. Evidence that supports oxidizing fluids includes veining[19], overprinting of palaeomagnetic signatures[20,21] and the resetting of isotope systems[22–24]. However, those studies are focused on areas proximal to high-grade ore deposits with a limited areal extent (Supplementary Information). To investigate the potential for oxidizing BIFs at a basin scale, we developed a simple hydrogeological box model

[1]Department of Earth & Atmospheric Sciences, University of Alberta, Edmonton, Alberta, Canada. [2]School of Natural and Environmental Sciences, Newcastle University, Newcastle upon Tyne, UK. [3]China University of Geosciences, State Key Laboratory of Geological Processes and Mineral Resources, Beijing, China. [4]Key Laboratory of Mineral Resources, Institute of Geology and Geophysics, Chinese Academy of Sciences, Beijing, China. [5]European Institute for Marine Studies, CNRS-UMR6538 Laboratoire Géosciences Océan, Technopôle Brest-Iroise, Plouzané, France. [6]Paleoproterozoic Mineralization Research Group, Department of Geology, University of Johannesburg, Johannesburg, South Africa. [7]Department of Science and Technology – National Research Foundation Centre of Excellence for Integrated Mineral and Energy Resource Analysis, Department of Geology, University of Johannesburg, Johannesburg, South Africa. [8]Present address: Department of Geology and Geophysics, Yale University, New Haven, CT, USA.
*e-mail: lrobbins@ualberta.ca

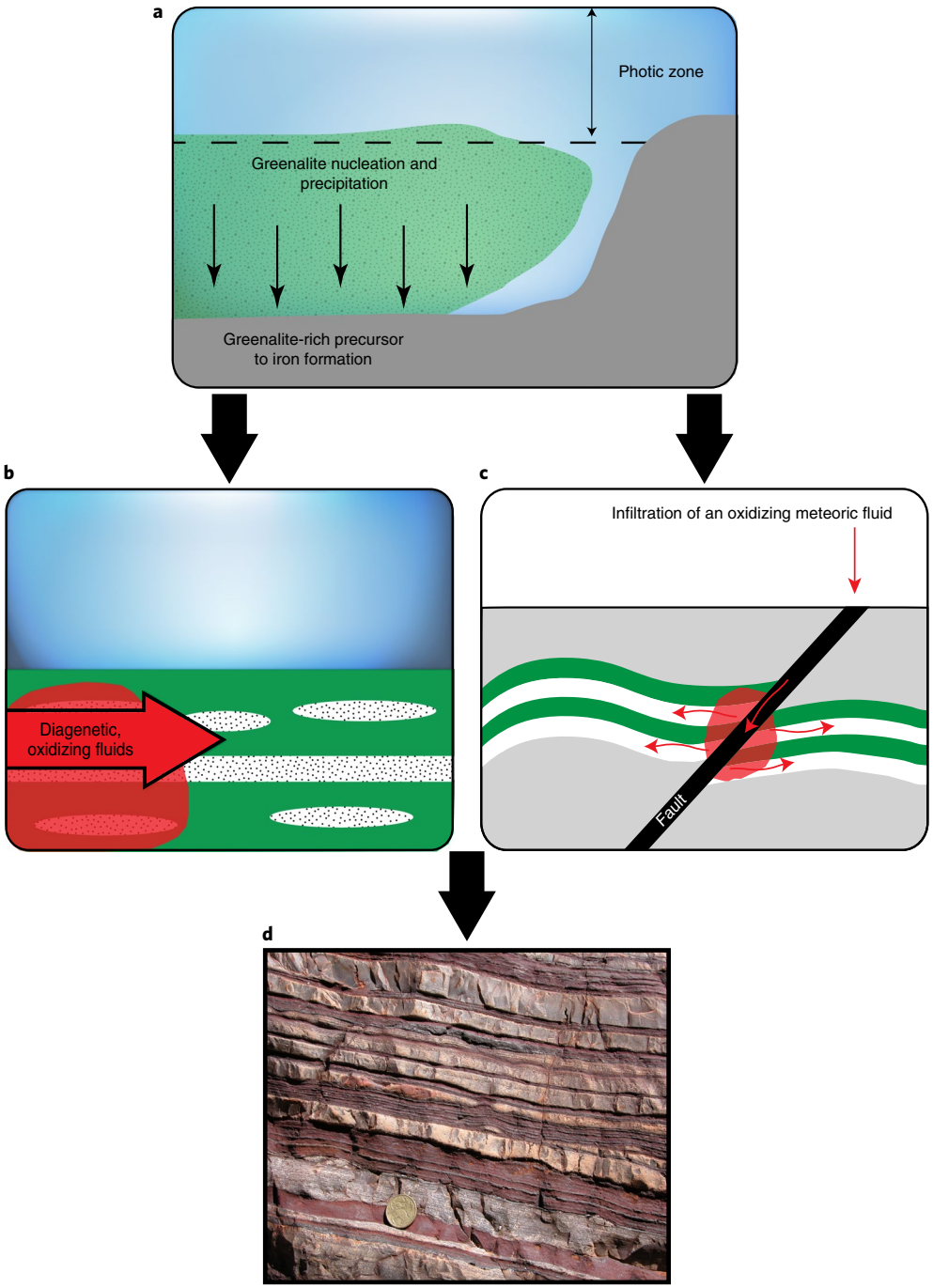

Fig. 1 | Conceptual model for the postdepositional oxidation of greenalite by oxidative groundwater (for example, Rasmussen et al.[14] and Johnson et al.[15]). **a**–**c**, Deposition of a greenalite precursor phase (**a**) followed by postdepositional oxidation pathways that include early diagenetic fluids (**b**) or infiltration of a meteoric oxidizing fluid and flow parallel to iron-rich layers (**c**) (as proposed by ref. [29]). **d**, Banding preserved in the Joffre Member of the Brockman Iron Formation, Western Australia. Any postdepositional oxidation must be capable of explaining the preservation of the distinct banding characteristic of BIFs.

(Fig. 2) to test the time needed to postdepositionally oxidize a deposit the size of the Hamersley Basin.

Postdepositional oxidation by groundwater

Oxidation time calculations were carried out by varying the (1) target percentage of Fe(II) oxidized, (2) permeability, (3) hydraulic gradient and (4) dissolved oxygen concentration (C_{DO}) (Table 1). A total of 51 different Fe tonnages, 36 different hydraulic conductivities, 19 different gradients and 109 different dissolved O_2 concentrations were considered, which resulted in 3,802,356 permutations. A permutation was considered successful if the time necessary for the oxidation was less than 250 Myr, the length of time between deposition and the Ophthalmian orogeny, or less than the minimum age of the BIF in the Hamersley Basin, ~2.45 Ga (ref. [25]). We also note that 250 Myr is considerably longer than the 70 Myr used by Rasmussen et al.[23] to explain an oxidation event purported to have affected most of the Hamersley Basin. Similarly, scenarios that account for the 1.3 Gyr of episodic hydrothermal alteration,

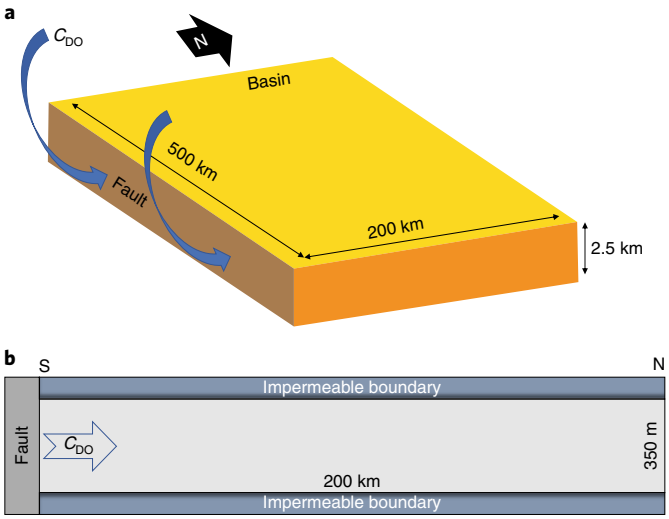

Fig. 2 | Geometry of the Hamersley Basin BIF. a, Dimensions and water infiltration along the major axis mimic the generalized fault distribution in a simplified view of the Hamersley Province (not to scale)[28,29]. **b**, Boundary conditions for the hydrogeological box model, which assumes a homogeneous, isotropic media with impermeable boundaries on the top, bottom and two lateral faces (not to scale).

Table 1 | Upper and lower limits for the parameters varied in hydrogeological box model simulations

Parameter	Lower limit	Upper limit	Number of steps
Percentage of iron mass (10^{17} kg) oxidized (%)	10	60	51
Permeability (m^2)[a]	2×10^{-16}	1×10^{-12}	36
Hydraulic gradient ($m\,m^{-1}$)[b]	0.001	0.1	19
Dissolved oxygen ($mg\,l^{-1}$)	0.00008	8	109

The ranges selected encompass a wide set of possible conditions. [a]From McLellan et al.[29]. [b]Assumed.

proposed to have grown new xenotime or reset its U–Pb isotope system[24], are encompassed within our 2.45 Gyr secondary cutoff. In other words, in constraining the model predictions, we erred on the conservative side. Of the 3,802,356 simulations run, only 40,251 (~1.06%) returned oxidation times <250 Myr (Fig. 3a). Of all the model runs, only 8.87% returned ages less than the age of the BIF themselves, 2.45 Gyr.

The fastest simulation required only 34.7 Myr. However, this specific model run utilized the highest permeability in the input range, greatest C_{DO}, largest topographic gradient and considered the oxidation of the least amount of Fe. Although that value of permeability is found in some limestones, dolostones and certain fractured basement rocks, as well as unconsolidated silt to silty sand[26], it is unlikely to be found consistently across a basin-scale flow system. Inherently, this makes this specific model run the most favourable, and a fast oxidation time was expected. The ~1.06% of runs that returned oxidation times <250 Myr share several informative commonalities. All required dissolved O_2 in excess of 1.2 $mg\,l^{-1}$ (compared to ~8 $mg\,l^{-1}$ for fully oxygenated freshwater) and a permeability >2×10^{-13} m^2 (compared to ~2×10^{-12} m^2 for sandstone) (Fig. 3b) and a hydraulic gradient (topographic slope) greater than 0.02 $m\,m^{-1}$. Each of these parameters are near the upper end of their ranges (Table 1 and Fig. 3b), and the possibility of them co-existing over hundreds of kilometres is remote. Similarly, simulations requiring less than 2.45 Gyr to oxidize the iron require high permeability and dissolved O_2 contents (Fig. 3b). Based on the results, we argue that dissolved O_2 introduced via groundwater flow acting on a basin-scale is highly implausible, requiring fluxes, dissolved O_2 concentrations, and permeability conditions that are unrealistically high. Furthermore, the inclusion of heterogeneities and/or anisotropy within the formation, and/or cross-formational leakage of water into other geological units, would greatly increase the time required to oxidize the formation.

Using parameters that are more representative of a large sedimentary basin, regional permeability = 2×10^{-16} m^2, hydraulic gradient = 0.003, dissolved oxygen = 0.1 $mg\,l^{-1}$ and a formation with a total iron tonnage of ~1×10^{17} kg (Bekker et al.[2]), we ran a single simulation for 250 Myr to estimate how much Fe(II) could be oxidized and what the horizontal penetration depth would be (Supplementary Fig. 2). The chosen permeability and hydraulic gradient values are consistent with basin-scale observations from the well characterized Alberta sedimentary basin, which is of comparable size[27]. This simulation demonstrated that, within the allotted 250 Myr, ~5.6×10^9 kg of Fe(II) could be oxidized, equivalent to only a very small fraction of the mass of the BIF within the Hamersley Basin. This resulted in a uniform 'penetration depth' of 1.08 cm along the fault. Although it is known that areas of the basin were affected by supergene alteration[28], it is likely that these areas represent a unique set of conditions that do not apply to a basin that spans 100,000 km^2.

Further considerations on BIF deposition

Although the hydrogeological model of McLellan et al.[29] might explain the alteration of BIF to ore bodies in some small, localized areas of the basin (for example, Brown et al.[19]), it is simply not feasible to extrapolate to the entirety of the Hamersley Basin because the extent of alteration evoked in this model is significantly smaller. Although overpressure may drive fluid flow during orogenic uplift, the effects of alteration are likely to be restricted to within a few tens of kilometres around the area of deformation, and fluid flow is expected to dissipate over thousands to tens of thousands of years[30–32]. Moreover, the characteristic products of alteration, microplaty haematite and martite (haematite pseudomorphs that replace magnetite), are not pervasive across the Hamersley Basin[33]. It is also difficult to envision a strongly oxygenated groundwater source in the Palaeoproterozoic given the low levels of atmospheric pO_2 (<10^{-5} to <0.1 of present atmospheric levels) during the onset of the GOE[34]. The likelihood for penetration of oxygenated groundwater into fractures, and the translation of these fluids to depth is also unclear. In modern shelf sediments, oxygen only penetrates to a few centimetres in depth[35], and groundwater also tends to fall towards reducing conditions[36].

Aside from the hydrogeological considerations presented here, there are several arguments against the greenalite hypothesis. First, immediately after deposition, it would have been difficult for sediments to become exposed to oxygenated waters because the Palaeoproterozoic deep ocean was anoxic and ferruginous[37,38]. A general lack of Ce/Ce* anomalies in BIFs prior to 1.9 Ga indicates that seawater remained dominantly anoxic even after the GOE[38]. In areas of supergene alteration and ore formation, Ce anomalies may develop as a result of the alteration within the ore bodies, even if the precursor BIF lacked true negative Ce anomalies[39]. Further, if O_2 had reached measurable concentrations at the seafloor, it would almost certainly have been consumed by the heterotrophic respiration of organic matter and could not have penetrated the sediment. These considerations highlight the difficulty in postdepositionally oxidizing Fe(II) immediately after the deposition at the sediment–water interface before any potential regional and/or tectonically induced groundwater flow.

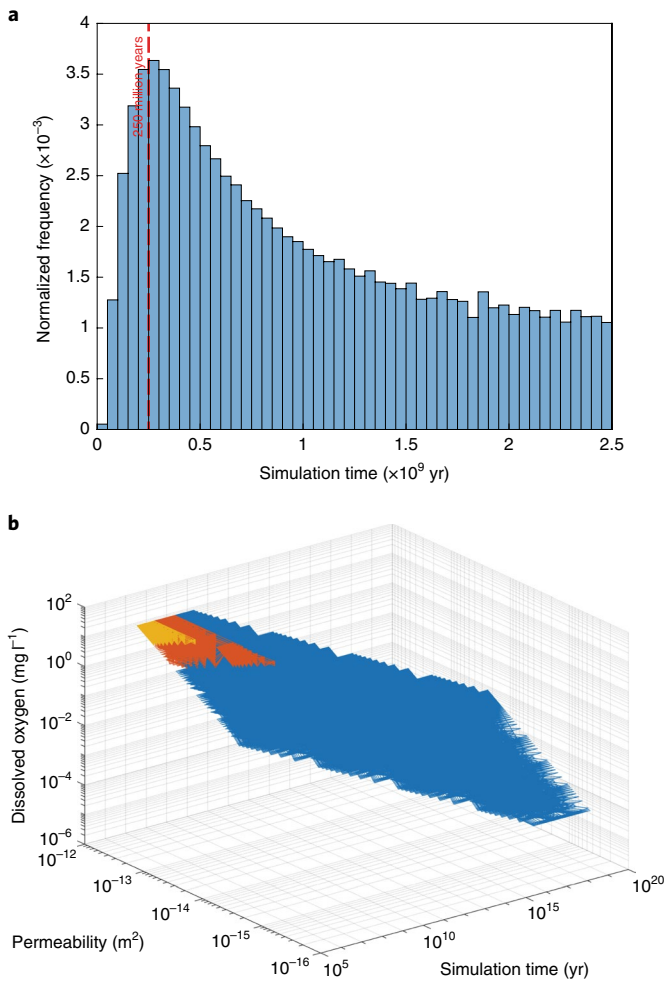

Fig. 3 | Distribution of simulation times for groundwater to oxidize the Hamersley Basin BIF. a, Normalized frequency for ~8.87% of 3,802,356 total model runs that return oxidation times less than 2.45 Gyr. Red line marks the 250 Myr cut-off described in the text. Only ~1.06% of the model runs required less than 250 Myr to oxidize 10–60% of the BIF in the Hamersley Basin. **b**, Three-dimensional view of the simulation times. Red, simulations that require <250 Myr; yellow, simulations that require <2.45 Gyr; blue, simulations that require oxidation times greater than the age of the Hamersley Basin.

Second, the Turee Creek Group (2.45–2.22 Ga) was deposited immediately over the Hamersley Group in a conformable ~3.9 km succession[3,40]. Sedimentation of this package would not only have prevented subaerial exposure and the infiltration of meteorically derived fluids, but would have contributed to the compaction of the BIF sediments hosted in the underlying Hamersley Group. Given the high permeability (1×10^{-12} m^2) required for the models to return oxidation times <250 Myr (Table 1 and Fig. 3), which are characteristic of unconsolidated fine-grained sands or silt[26], the deposition of the Turee Creek Group represents a significant obstacle to maintaining the conditions necessary for the flow of oxygenated groundwater. Crucially, correlations of the Hamersley Group BIF to those of the Transvaal Supergroup indicate that these deposits may have originally been deposited within adjacent sub-basins[1] (Supplementary Information). Therefore, any postdepositional alteration would have had to affect both sub-basins in a similar manner over an even larger areal extent than considered in our model. By extension, similar postdepositional processes would be required to account for all the major BIFs deposited during the Archaean–Palaeoproterozoic transition, which include the Kursk Supergroup (Russia), Krivoy Rog Supergroup (Ukraine), Cauê Formation (Brazil), Benchmark Iron Formation (USA) and the Ruker Series (Antarctica). It is implausible that every basin would have had the hydrogeological conditions for greenalite to be oxidized postdepositionally by groundwater.

Third, Lake Superior-type BIFs like those of the Hamersley and Transvaal basins have characteristic millimetre-scale microbands and centimetre-scale mesobands[2,11]. McLellan et al.[29] proposed that infiltration of the heated, meteoric fluid would have obliterated these layers, which would increase the permeability of the BIF units and thus facilitate oxidation as well as the emplacement of microplaty haematite. Although this process may be responsible for upgrading the initial BIF to ore bodies, it is unlikely to apply to formations where millimetre- and centimetre-scale Fe- and silica-rich bands are characteristically preserved, such as in the Brockman Iron Formation, the quintessential BIF by which banding was defined[41].

Fourth, the preservation of seawater-like rare earth element patterns suggests that any fluid alteration occurred at low water-to-rock ratios[42], and thereby requires either higher oxygen concentrations or longer timescales for the postdepositional oxidation of Fe(II), both of which argue against the rapid postdepositional oxidation of a greenalite precursor. In ore bodies, supergene alteration leads to heavy rare earth element depletion, a geochemical characteristic not typical of oxide, carbonate or silicate facies BIFs[39]. Other geochemical indicators, such as Fe- and Si-isotope heterogeneities, are also at odds with the large-scale obliteration of the primary mineralogy and suggest at least a partial oxidation of Fe(II) in surface waters[43,44] or that the primary Fe-bearing precipitate was an Fe(III)–Si gel[45].

Below we outline the possible origins for greenalite that decouple its formation from the water column. The precipitation of greenalite requires high Fe, high Si and a mildly alkaline pH. These factors can all be satisfied during early diagenesis within an HFO sediment pile. The Fe(III) and silica are first delivered to the sediments as an HFO particle with silica adsorbed to its surface, that is, a water column Fe–Si shuttle[46]. The HFO is then reduced to dissolved Fe(II) via dissimilatory iron reduction, which also generates mildly alkaline pH conditions via the reaction:

$$CH_3COO^- + 8Fe(OH)_3 \leftrightarrow 8Fe^{2+} + 2HCO_3^- + 15OH^- + 5H_2O$$

The bicarbonate generated could form carbonates or be effluxed back to the water column. Similarly, a benthic Fe shuttle[47] may explain the origins of greenalite, in which Fe(II) is liberated from the HFO deposited on the shelf through dissimilatory iron reduction or reductive dissolution and transported either with groundwater or in the water column to localized environments where greenalite could precipitate. Another possibility is that greenalite formed in sediment pore waters through reverse weathering, a process recently proposed to act as a long-term climate and marine pH stabilizer in the absence of silica-secreting organisms[48].

Finally, an alternative possible origin for greenalite is indicated by the greenalite-rich and chert-poor lithofacies in the shallow-water deposits of the Transvaal Supergroup (Supplementary Information). A shallow water origin for greenalite is indicated by the increased textural evidence for wave reworking observed in the Westerberg Member and interbedding with granular iron formation[49]. Evaporation may have led to the supersaturation of Fe(II) in restricted settings, in which Si concentrations were depressed due to chert precipitation in deeper water, which created conditions favourable for greenalite precipitation. The greenalite could then be brought into BIF depositional basins by currents. Although silicate facies BIF may contain appreciable greenalite, this does not apply to the oxide facies BIF discussed here, where it is the

exception. Critically, whether deposited as an early diagenetic pore-water phase or as a distinct phase formed in restricted environments, it is highly probable that greenalite was not a precursor mineral phase to archetypal BIF deposition.

As demonstrated through realistic constraints and a simple box-modelling approach, the time required to postdepositionally oxidize an aerially extensive BIF is unreasonable. By contrast, the interpretation of an HFO precursor is consistent with the generally accepted involvement of either cyanobacteria or anoxygenic photoferrotrophs as the mechanism that underpins BIF deposition, as well as the trace element and isotope geochemistry of BIFs. Indeed, greenalite as the precursor mineral to BIFs would indicate an absence of oxidizing agents in seawater at 2.45 Ga, a concept difficult to accept given that this time corresponds to the rise of atmospheric oxygen—the GOE. Although the localized precipitation of greenalite cannot be ruled out, results from this study suggest that the greenalite in oxide facies BIFs is more consistent with being an early diagenetic phase, rather than a primary depositional component that necessitates a significant departure from our current understanding of Archaean–Palaeoproterozoic seawater chemistry.

Online content

Any methods, additional references, Nature Research reporting summaries, source data, statements of code and data availability and associated accession codes are available at https://doi.org/10.1038/s41561-019-0372-0.

Received: 1 July 2018; Accepted: 13 April 2019;
Published online: 27 May 2019

References

1. Beukes, N. J. & Gutzmer, J. Origin and paleoenvironmental significance of major iron formations at the Archean–Paleoproterozoic boundary. *SEG Rev.* **15**, 5–47 (2008).
2. Bekker, A. et al. in *Sediments, Diagenesis and Sedimentary Rocks* 2nd edn (ed. Mackenzie, F. T.) 561–628 (Elsevier, 2014).
3. Trendall, A. F. & Blockley, J. G. The iron formations of the Precambrian Hamersley Group Western Australia with special reference to the associated crocidolite. *Geol. Surv. West. Aust. Bull.* **119**, 1–366 (1970).
4. Morris, R. Genetic modelling for banded iron-formation of the Hamersley Group, Pilbara Craton, Western Australia. *Precambrian Res.* **60**, 243–286 (1993).
5. Konhauser, K. O. et al. Aerobic bacterial pyrite oxidation and acid rock drainage during the Great Oxidation Event. *Nature* **478**, 369–373 (2011).
6. Gumsley, A. P. et al. Timing and tempo of the Great Oxidation Event. *Proc. Natl Acad. Sci. USA* **114**, 1811–1816 (2017).
7. Farquhar, J., Zerkle, A. L. & Bekker, A. Geological constraints on the origin of oxygenic photosynthesis. *Photosynth. Res.* **107**, 11–36 (2011).
8. Cloud, P. E. Significance of the Gunflint (Precambrian) microflora. *Science* **148**, 27–35 (1965).
9. Konhauser, K. O. et al. Could bacteria have formed the Precambrian banded iron formations? *Geology* **30**, 1079–1082 (2002).
10. Posth, N. R., Canfield, D. E. & Kappler, A. Biogenic Fe(III) minerals: from formation to diagenesis and preservation in the rock record. *Earth Sci. Rev.* **135**, 103–121 (2014).
11. Konhauser, K. O. et al. Iron formations: a global record of Neoarchaean to Palaeoproterozoic environmental history. *Earth Sci. Rev.* **172**, 140–177 (2017).
12. Rasmussen, B., Krapez, B. & Meier, D. B. Replacement origin for hematite in 2.5 Ga banded iron formation: evidence for postdepositional oxidation of iron-bearing minerals. *Geol. Soc. Am. Bull.* **126**, 438–446 (2014).
13. Rasmussen, B., Muhling, J. R., Suvorova, A. & Krapez, B. Dust to dust: evidence for the formation of 'primary' hematite dust in banded iron formations via oxidation of iron silicate nanoparticles. *Precambrian Res.* **284**, 49–63 (2016).
14. Rasmussen, B., Muhling, J. R., Suvorova, A. & Krapez, B. Greenalite precipitation linked to the deposition of banded iron formations downslope from a late Archean carbonate platform. *Precambrian Res.* **290**, 49–62 (2017).
15. Johnson, J. E., Muhling, J. R., Cosmidis, J., Rasmussen, B. & Templeton, A. S. Low-Fe(III) greenalite was a primary mineral from Neoarchean oceans. *Geophys. Res. Lett.* **45**, 3182–3192 (2018).
16. Konhauser, K. O. et al. Oceanic nickel depletion and a methanogen famine before the Great Oxidation Event. *Nature* **458**, 750–753 (2009).
17. Planavsky, N. J. et al. The evolution of the marine phosphate reservoir. *Nature* **467**, 1088–1090 (2010).
18. Konhauser, K. O. et al. Phytoplankton contributions to the trace-element composition of Precambrian banded iron formations. *Geol. Soc. Am. Bull.* **130**, 941–951 (2018).
19. Brown, M. C., Oliver, N. & Dickens, G. R. Veins and hydrothermal fluid flow in the Mt. Whaleback iron ore district, eastern Hamersley Province, Western Australia. *Geochim. Cosmochim. Acta*. **128**, 441–474 (2004).
20. Schmidt, P. W. & Clark, D. A. Palaeomagnetism and magnetic anisotropy of Proterozoic banded-iron formations and iron ores of the Hamersley Basin, Western Australia. *Precambrian Res.* **69**, 133–155 (1994).
21. Tompkins, L. A. & Cowan, D. R. Opaque mineralogy and magnetic properties of selected banded iron-formations, Hamersley Basin, Western Australia. *Aust. J. Earth Sci.* **48**, 427–437 (2010).
22. Alibert, C. & McCulloch, M. Rare earth element and neodymium isotopic compositions of the banded iron-formations and associated shales from Hamersley, Western Australia. *Geochim. Cosmochim. Acta* **57**, 187–204 (1993).
23. Rasmussen, B., Fletcher, I. R. & Sheppard, S. Isotopic dating of the migration of a low-grade metamorphic front during orogenesis. *Geology* **33**, 773–776 (2005).
24. Rasmussen, B., Fletcher, I., Muhling, J., Thorne, W. & Broadbent, G. Prolonged history of episodic fluid flow in giant hematite ore bodies: evidence from in situ U–Pb geochronology of hydrothermal xenotime. *Earth Planet. Sci. Lett.* **258**, 249–259 (2007).
25. Warchola, T. et al. Petrology and geochemistry of the Boolgeeda Iron Formation, Hamersley Basin, Western Australia. *Precambrian Res.* **316**, 155–173 (2018).
26. Freeze, R. A. & Cherry, J. A. *Groundwater* (Prentice-Hall, 1979).
27. Adams, J. J., Rostron, B. J. & Mendoza, C. A. Coupled fluid flow, heat and mass transport, and erosion in the Alberta basin: implications for the origin of the Athabasca oil sands. *Can. J. Earth Sci.* **41**, 1077–1095 (2004).
28. Powell, C. M., Oliver, N. H. S., Li, Z.-X., Martin, D. M. & Ronaszeki, J. Synorogenic hydrothermal origin for giant Hamersley iron oxide ore bodies. *Geology* **27**, 175–178 (1999).
29. McLellan, J. G., Oliver, N. H. S. & Schaubs, P. M. Fluid flow in extensional environments; numerical modelling with an application to Hamersley iron ores. *J. Struct. Geol.* **26**, 1157–1171 (2004).
30. Ge, S., & Garven, G. in *Origin and Evolution of Sedimentary Basins and their Energy and Mineral Resources* (ed. Price, R. A.) 145–157 (AGU, 1989).
31. Ge, S. & Garven, G. Hydromechanical modeling of tectonically driven groundwater flow with application to the Arkoma Foreland Basin. *J. Geophys. Res.* **97**, 9119–9144 (1992).
32. Ge, S. & Garven, G. A theoretical model for thrust-induced deep groundwater expulsion with application to the Canadian Rocky Mountains. *J. Geophys. Res.* **99**, 13851–13868 (1994).
33. Haugaard, R., Pecoits, E., Lalonde, S. V., Rouxel, O. J. & Konhauser, K. O. The Joffre banded iron formation, Hamersley Group, Western Australia: Assessing the palaeoenvironment through detailed petrology and chemostratigraphy. *Precambrian Res.* **273**, 12–37 (2016).
34. Lyons, T. W., Reinhard, C. T. & Planavsky, N. J. The rise of oxygen in Earth's early ocean and atmosphere. *Nature* **506**, 307–315 (2014).
35. Canfield, D. E. et al. Pathways of organic carbon oxidation in three continental margin sediments. *Mar. Geol.* **113**, 27–40 (1993).
36. Becking, L. & Kaplan, I. R. Limits of the natural environment in terms of pH and oxidation–reduction potentials. *J. Geol.* **68**, 243–284 (1960).
37. Poulton, S. W. & Canfield, D. E. Ferruginous conditions: a dominant feature of the ocean through Earth's history. *Elements* **7**, 107–112 (2011).
38. Planavsky, N. et al. Rare earth element and yttrium compositions of Archean and Paleoproterozoic Fe formations revisited: new perspectives on the significance and mechanisms of deposition. *Geochim. Cosmochim. Acta* **74**, 6387–6405 (2010).
39. Smith, A. J. B. & Beukes, N. J. Paleoproterozoic banded iron formation-hosted high grade hematite iron ore deposits of Transvaal Supergroup, South Africa. *Episodes* **39**, 269–284 (2016).
40. Van Kranendonk, M. J. & Mazumder, R. Two Paleoproterozoic glacio-eustatic cycles in the Turee Creek Group, Western Australia. *Geol. Soc. Am. Bull.* **127**, 596–607 (2015).
41. Trendall, A. F. Progress report on the Brockman Iron Formation in the Wittenoom-Yampire Area. *West. Aust. Geol. Surv. Ann. Rep.* **1964**, 55–65 (1964).
42. Bau, M. Effects of syn- and post-depositional processes on the rare-earth element distribution in Precambrian iron-formations. *Eur. J. Mineral.* **5**, 257–267 (1993).
43. Johnson, C. M., Beard, B. L., Klein, C., Beukes, N. J. & Roden, E. E. Iron isotopes constrain biologic and abiologic processes in banded iron formation genesis. *Geochim. Cosmochim. Acta* **72**, 151–169 (2008).
44. Steinhoefel, G. et al. Deciphering formation processes of banded iron formations from the Transvaal and the Hamersley successions by combined Si and Fe isotope analysis using UV femtosecond laser ablation. *Geochim. Cosmochim. Acta* **74**, 2677–2696 (2010).

45. Percak-Dennett, E. M. et al. Iron isotope fractionation during microbial dissimilatory iron oxide reduction in simulated Archaean seawater. *Geobiology* **9**, 205–220 (2011).
46. Fischer, W. & Knoll, A. H. An iron shuttle for deepwater silica in Late Archean and early Paleoproterozoic iron formation. *Geol. Soc. Am. Bull.* **121**, 222–235 (2009).
47. Li, W., Beard, B. L. & Johnson, C. M. Biologically recycled continental iron is a major component in banded iron formations. *Proc. Natl Acad. Sci. USA* **112**, 8193–8198 (2015).
48. Isson, T. T. & Planavsky, N. J. Reverse weathering as a long-term stabilizer of marine pH and planetary climate. *Nature* **560**, 471–475 (2018).
49. Beukes, N. Sedimentology of the Kuruman and Griquatown iron-formations, Transvaal supergroup, Griqualand West, South Africa. *Precambrian Res.* **24**, 47–84 (1984).

Acknowledgements

L.J.R. acknowledges a NSERC Vanier Canada Graduate Scholarship and T.J.W. a NSERC CGS-M. This work was supported by NSERC Discovery Grants to K.O.K. (RGPIN-165831) and D.S.A. (RGPIN-04134). N. MacPherson and W. Hao are thanked for thoughtful discussions and input on an early draft.

Author contributions

L.J.R., K.O.K. and D.S.A. designed the study, and L.J.R., S.P.F., K.O.K., D.S.A. and B.J.R. designed and evaluated the hydrogeological model. A.J.B.S. and N.J.B. provided the geological context that aided the interpretation of the model. All the authors contributed to the interpretation and writing of the manuscript.

Competing interests

The authors declare no competing interests.

Additional information

Supplementary information is available for this paper at https://doi.org/10.1038/s41561-019-0372-0.

Reprints and permissions information is available at www.nature.com/reprints.

Correspondence and requests for materials should be addressed to L.J.R.

Publisher's note: Springer Nature remains neutral with regard to jurisdictional claims in published maps and institutional affiliations.

Methods

The proposed mechanism for the oxidation of greenalite in BIFs invoked by Rasmussen et al.[12] utilizes a hydrogeological model[29] in which meteorically derived, O_2-bearing groundwater leads to the dissolution of silica layers and concurrent oxidation of the Fe(II)-rich layers (Fig. 1c). In the previous model[29], meteoric water infiltrated the Hamersley Basin BIF through fractures to a depth of ~2 km, with subsequent flow moving laterally along Fe(II)-rich strata over 10 km. This fluid flow is suggested to have occurred between 2.45 and 2.2 Ga, coincident to the Ophthalmian orogeny[28,29].

Our model seeks to test whether pervasive groundwater flow could be a reasonable mechanism for the secondary oxidation of BIFs on a basin scale by employing a series of simulations to test whether the time required to introduce sufficient quantities of dissolved oxygen to oxidize a mass of Fe(II) in the system is reasonable. We employed a simple box model because the first-order groundwater and mass transport conditions approximated by such a model must be plausible to justify pursuing a more complex numerical analysis, such as a coupled solute–heat–groundwater flow model. As demonstrated below, a more detailed model was not necessary.

To determine whether a simulation was successful, the calculated time to introduce sufficient quantities of oxygen to oxidize the amount of Fe(II) considered had to be equal to, or less than, 250 Myr, the amount of time between deposition and the 2.2 Ga Ophthalmian orogeny, a critical event for the postdepositional oxidation of these BIF units[28,29]. Taking a broader view, 2.45 Gyr was used as a secondary cutoff as this corresponds to the minimum age of the BIF in the Hamersley Basin[25]. Based on the spatial distribution of the basin[28,29], we simplified the geometry of the Hamersley Basin to a rectangular prism, with a width of 500 km, a length of 200 km and a total thickness of 2.5 km (Fig. 2a). Based on the stratigraphy of the Palaeoproterozoic Hamersley Basin, we conservatively estimated that the iron-rich layers may be represented by a thickness of ~350 m and simplified our box model accordingly (Fig. 2b); at a constant density, this resulted in a total tonnage at least 10^{17} kg (ref. [2]). We assumed that the water flowed into the formation from the southern edge via the major faults within the formation (Fig. 2a). Under the idealized conditions for model success, the fault was assumed to be uniform, continuous, fully penetrating and delivered a constant flow of water. Flow and transport were assumed to be horizontal and one-dimensional. The formation was assumed to be a homogeneous and isotropic mass of Fe(II), with impermeable boundaries on the top, bottom and two side faces (Fig. 2b). An instantaneous reaction whereby 1 mol of O_2 oxidizes 4 mol of Fe(II) was also used. The flow calculations were based on Darcy's Law:

$$Q = KA\frac{dh}{dx} \quad (1)$$

where Q is the volumetric flow rate (L^3T^{-1}) (L, length; T, time), K is the hydraulic conductivity (LT^{-1}), A is the cross-sectional area (L^2) and dh/dx is the hydraulic gradient (LL^{-1}). The hydraulic gradient for this basin was unknown and so was varied in the simulations. The lower limit was constrained based on typical topographic gradients found in geological basins[27] and varied between 0.001 and 0.1 m m^{-1} (Table 1). The hydraulic conductivity of the formation was calculated from the permeability of the formation[29] based on the relationship:

$$K = k\frac{\rho g}{\mu} \quad (2)$$

where k is the permeability (L^2), ρ is the density of water (assumed to be 1,000 kg m^{-3}), g *is* the acceleration due to gravity (assumed to be 9.81 m s^{-2}) and μ is the viscosity of water (assumed to be 1×10^{-3} Pa s). Permeability was varied between 2×10^{-16} and 1×10^{-12} m^2 (Table 1), which represents a reasonable subset of the range examined by McLellan et al.[29].

A key unknown parameter is the concentration of dissolved oxygen in the water. Using Henry's Law as a guide, and correcting for the effect of temperature[50] and the abundance of oxygen in the atmosphere at the time[34], we determined that a realistic range of dissolved oxygen could be between 8 mg l^{-1} (modern freshwater exposed to the atmosphere) and 0.00008 mg l^{-1} (concentrations in equilibrium with the atmosphere just prior to the GOE, assuming atmospheric O_2 levels of 10^{-5} times present) (Table 1). The concentration of dissolved oxygen introduced into the formation was assumed to be constant throughout a simulation. We calculated the time necessary to oxidize between 10 and 60% of the 10^{17} kg of Fe, as BIFs have an average oxidation state of $Fe^{2.4+}$ when both the ferrous and ferric phases are considered[51], but have undergone some level of dissimilatory iron reduction; this represents only a fraction of the total mass of the Hamersley Basin[2,11].

First, we calculated the flux of water through the BIF for a range of hydraulic gradients and permeabilities, as outlined in Table 1. We then calculated the time needed to introduce a sufficient flux of oxygen to oxidize the requisite amount of Fe(II) given a range of C_{DO} (Table 1). By varying these four parameters through their respective ranges, 3,802,356 permutations were considered in our box model.

Knowing the volumetric flow rate Q into the formation, the mass of Fe in the system, and assuming C_{DO} (ML^{-3}) (M, mass), we then determined the mass flow rate of oxygen (MT^{-1}) by equation (3) and the reaction time t (T) by equation (4):

$$\dot{M} = QC_{DO} \quad (3)$$

$$t = \frac{m}{\dot{M}} \quad (4)$$

Where m is the mass of oxygen required to oxidize the Fe in the system (M). Knowing the mass of iron in the system[2], we calculated the time (t) required to oxidize that mass (m) using the calculated mass flow rate ($\dot{M}$) of oxygen.

Data availability

All data supporting this study are included in the manuscript and Supplementary Information.

Code availability

The customized MATLAB code used for the hydrogeological box model calculations is available in the Supplementary Information. The equations and values that underlie the calculations are described in detail in Methods.

References

50. Sander, R. *Compilation of Henry's Law Constants for Inorganic and Organic Species of Potential Importance in Environmental Chemistry* (Max-Planck Institute of Chemistry, 1999).
51. Klein, C. & Beukes, N. J. in *The Proterozoic Biosphere* (eds Schopf, J. W. & Klein, C.) 139–146 (Cambridge Univ. Press, 1992).